Electronic Supplementary Material (ESI) for Soft Matter.
This journal is © The Royal Society of Chemistry 2017

Evaluation of dextran(ethylene glycol) hydrogel films for giant unilamellar lipid vesicle production and their application for the encapsulation of polymersomes

Nestor Lopez Mora, Yue Gao, M. Gertrude Gutierrez, Justin Peruzzi, Ivan Bakker, Ruud J.R.W. Peters, Bianka Siewert, Sylvestre Bonnet, Roxanne E. Kieltyka,* Jan C. M. van Hest, Noah Malmstadt and Alexander Kros*

SUPPORTING INFORMATION

Contents: Page

1. Experimental Section

Synthesis and characterization of DexMal (**1**) with different degrees of substitution S2

Synthesis of PS-*b*-PEG polymersomes S4

2. General methods

Determination of mass swelling ratio S4

Cryo-scanning electron microscopy (cryo-SEM) S4

Oscillatory rheology S5

Flow cytometry (FACS) S5

Differential scanning calorimetry (DSC) S9

Confocal and differential interference contrast (DIC) imaging S11

3. References S13

1. Experimental Section

*Synthesis and characterization of **1** with different degrees of substitution.*

N-Maleoyl-β-alanine was prepared following a previously reported procedure for obtaining maleimido alkanoic acids.[1] Maleic anhydride (9.95 g) and β-Alanine (9.18 g) were added to acetic acid (75 mL). The mixture was refluxed at 170 °C for 90 minutes and subsequently, cooled to room temperature. The acetic acid was removed under reduced pressure. The residual acetic acid was further removed by forming an azeotrope with toluene under reduced pressure. The crude was extracted three times in ethyl acetate, the organic layer was dried with $MgSO_4$ and recrystallized from ethyl acetate at 4 °C overnight. The compound was further purified by sublimation using a cold finger. Yield = 31.6 %. ^{1}H-NMR (400MHz, $CDCl_3$): δ = 6.7 (s, -C**H**=C**H**-), 3.8 (HOOC-C**H**$_2$-CH$_2$), 2.7 (-CH$_2$-C**H**$_2$-N).

Polymer **1** was synthesized by N,N′-Diisopropylcarbodiimide mediated esterification of the hydroxyl groups of dextran with N-maleoyl-β-alanine. For a DS=4: dextran (0.62 g), N-maleoyl-β-alanine (0.42 g) and 4-(Dimethylamino)pyridinium 4-toluenesulfonate (DPTS) (0.15 g) were dissolved in anhydrous dimethyl sulfoxide (25 mL). The mixture was stirred at room temperature for two hours, followed by the addition of N,N′-Diisopropylcarbodiimide (0.48 mL). After stirring overnight (19 hours) at room temperature, the formed N, N'-dialkylurea was removed by filtration. The crude product was precipitated from cold isopropanol, dissolved in water and extensively dialyzed against Milli-Q water for two days before lyophilization. ^{1}H NMR (400 MHz, D_2O): δ = 3.3-4.0 (m, dextran glucopyranosyl ring protons), 4.9 (s, dextran anomeric proton), 6.8 (s, maleimide). ^{13}C NMR (400MHz, D_2O): δ= 134.5, 97.7, 73.4, 71.4, 69.5, 65.5.

The degree of substitution (DS) of **1** is defined as the number of maleimide groups per 100 glucopyranose residues of dextran, which was calculated from ^{1}H NMR spectra using the signals corresponding to the maleimide protons (δ 6.8) and anomeric proton of glucopyranose (δ 4.9). The DS of DexMal was controlled by the molar ratio between dextran and N-maleoyl-β-alanine as shown in *Fig. S1*. The conjugation of N-maleoyl-β-alanine to dextran was confirmed by the growth of FT-IR band at 1700 cm^{-1} belonging to the ester (*Fig. S2*). This band increases with the degree of substitution on the dextran, while the broad hydroxyl group band between 3000 - 3700 cm^{-1} is observed, indicating the presence free hydroxyl groups.

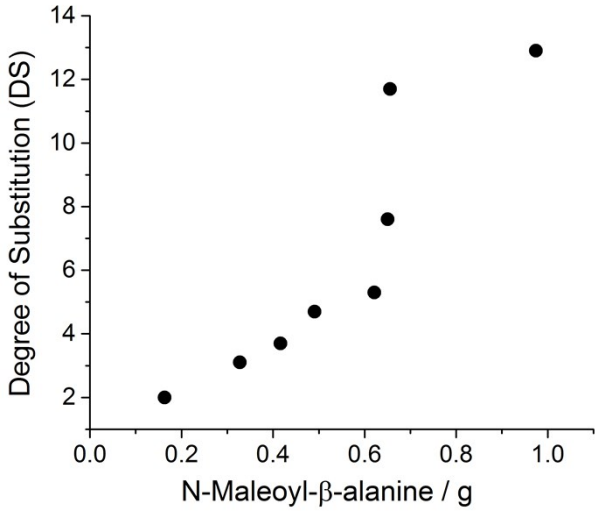

Fig. S1 Degree of substitution (DS) of **1** as a function of the mass of N-maleoyl-β alanine added. The degree of substitution (DS) is determined from the ^{1}H NMR.

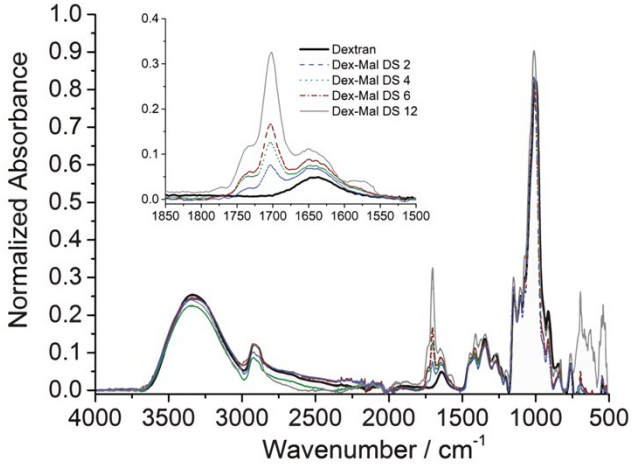

Fig. S2 FT-IR spectra of dextran and Dex-Mal (**1**) with various substitution degrees (DS = 2, 4, 6, 12). The inset image shows the increase of the ester band (1700 cm^{-1}) corresponding to the bond between dextran and N-maleoyl-β-alanine.

Synthesis of polystyrene-block-polyethylene glycol (PS-b-PEG) polymersomes.

Polymersomes were synthesized according to a previously described method.[2, 3] Briefly, PS_{300}-*b*-PEG_{44}-OMe and PS_{280}-*b*-PEG_{44}-Atto488 (5 wt%) polymers were dissolved in THF/dioxane (6:4, total volume 1 mL, 10 mg/mL) and stirred gently in a glass vial sealed with a rubber septum. Using a syringe pump (Harvard Apparatus), MilliQ water (3 mL, 1 mL/h flow rate) was slowly added to the polymer solution. After this, the turbid, slightly pink solution was transferred into a dialysis bag (SpectraPor, Breda, The Netherlands, MWCO 12 - 14 kDa) and dialysed against fresh MilliQ water for 24 hours, with regular changes of the external dialysis medium in order to remove residual organic solvent. After dialysis, the polymersomes were removed from the dialysis bag and stored in a glass vial. Characterization by dynamic light scattering produced a z-average diameter of 574 ±4.7 nm, with a PDI of 0.058 ± 0.05. PS300-PEG44–OMe and PS280-PEG44-Atto488 polymers were kindly provided by Joep van der Weijden and Silvie Meeuwissen (both Radboud University Nijmegen).

2. General Methods

Determination of mass swelling ratio. Various Dex-Mal polymers and PEG crosslinkers were dissolved in phosphate buffered saline (PBS, 150 mM, pH 7.4) respectively. For each tested hydrogel sample, 100 µL Dex-Mal solution and 100 µL corresponding PEG crosslinker were mixed together in a glass vial using a pipette at room temperature (22 °C). All samples were left overnight for fully gelation at room temperature, then 2 mL PBS buffer was added on top of each hydrogel sample. At various time points, each swollen hydrogel was weighed and fresh buffer was put on top afterwards. When the weight of swollen hydrogel reached a plateau, the mass swelling ratio was calculated using the equation $q_w = W_s/W_d$, where q_w is the mass swelling ratio of hydrogels after equilibrium swelling,W_s is the weight of equilibrium swollen hydrogel and W_d the weight of dry hydrogel. Each set of hydrogels were measured in triplicate.

Cryo-Scanning Electron Microscopy (cryo-SEM). The morphologies of the hydrogels in the swollen state were imaged in a JEOL 6330 Cryo Field Emission Scanning Electron Microscope from the General Instrumentation Facility at Radboud University (Nijmegen, The Netherlands). DexPEG hydrogel (5 µL volume) was injected into a hollow cylindrical sample holder and immediately flash frozen in liquid nitrogen. The sample was inserted in the cold-stage of the SEM cryo-preparation chamber and cleaved to make a horizontal fracture plane. The water was sublimated over 15 minutes and the fracture plane was coated with a thin gold-palladium layer. Subsequently, the sample was transferred into the SEM chamber, where it remained frozen during imaging.

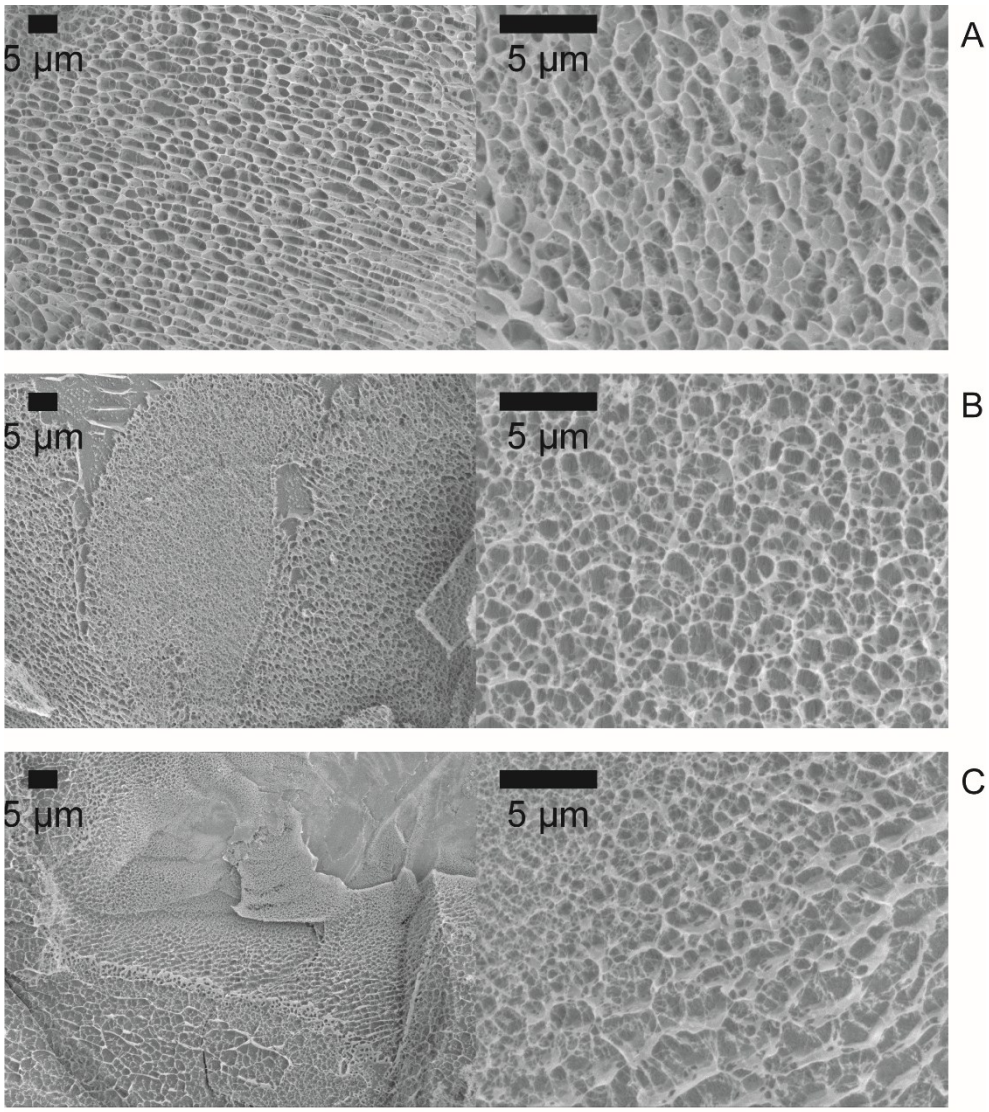

Fig. S3 Cryo-SEM of DexPEG hydrogels with different molar ratios between Dex-Mal (**1**) and PEG (**2**) precursors. A) Dex-Mal (**1** DS=4) – PEG (**2**) crosslinker (1:1 molar ratio). B) Dex-Mal (**1** DS=4) – PEG (**2**) crosslinker (1:0.75 molar ratio). C) DexMal (**1** DS=4) – PEG (**2**) crosslinker (1:0.5 molar ratio).

Oscillatory Rheology. Oscillatory time sweeps were performed on a Discovery Hybrid Rheometer (DHR-2) from TA Instruments using a plate – plate geometry. The precursors Dex-Mal (**1**) with various DS and thiolated PEG solutions (molecules **2** – **6**) were loaded on the lower plate and the upper plate (25 mm diameter) was immediately lowered to a gap distance of 0.5 mm. Oscillatory rheology time sweeps were performed on the various forming hydrogel materials by following the storage (G') and loss (G") moduli with respect to time at an angular frequency of 1 rad/s and 1% strain.

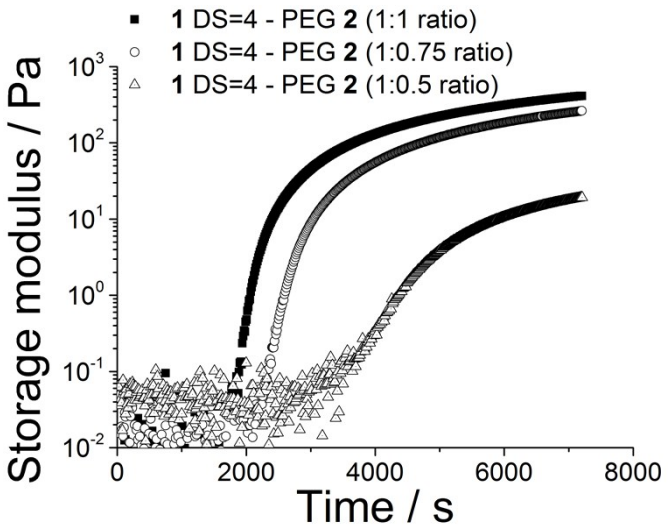

Fig. S4 Mechanical characterization of DexPEG hydrogels with increasing PEG cross-linker using oscillatory time sweeps. *Filled square*: Dex-Mal (**1** DS=4) – PEG (**2**) 1:1 molar ratio, *Hollow circle*: Dex-Mal (**1** DS=4) – PEG (**2**). 1:0.75 molar ratio, *Hollow triangle:* Dex-Mal (**1** DS=4) – PEG (**2**), 1:0.5 molar ratio.

Flow Cytometry. A Beckman Coulter Quanta instrument was used to analyze the yield and the size distribution of several GUV batches. In contrast to common fluorescence flow cytometers, which only depend on optical parameters, *i.e.* light scattering and fluorescence, the employed Beckman Coulter system additionally utilizes electrical impedance, also known as Coulter Principle.[4, 5] Briefly, particles pass through the orifice of a saline-filled cell. A constant (DC) current is applied across this aperture with an electrical circuit. Whenever the nonconductive GUVs pass through this orifice a voltage pulse will be generated.[2, 5] The amplitude thereof is theoretically proportional to the volume of the particles, and expressed as electric volume (*EV*). Based on the Coulter Principle, an accurate size measurement can be guaranteed, as the *EV* is in contrast to the forward scatter (*FSC*) monotonic.[6] In addition and simultaneously, each particle is irradiated by a 488 nm laser beam enabling the detection of side scatter (*SSC*), and therewith the density of the investigated particles, as well as fluorescence (available filters: 525 BP (*FL1*), 575 BP (*FL2*), 670 LP (*FL3*)).

Labelling of the lipid membrane of GUVs with DOPE-NBD ($\lambda_{max,\ abs}$ = 460 nm, $\lambda_{max,\ em}$ = 535 nm) allowed a clear distinction between sample and background or noise signals. A suspension of freshly prepared GUVs (500 µL) was gently mixed, transferred to a 24 well plate and placed in the auto sampler of the Beckman Coulter Quanta

instrument. Before injecting the suspension (50 µL), the 24 well plate was orbitally shaken to avoid biases due to the settlement of GUVs and prevent their damage by harsh suspension through a syringe. The *EV*, *SSC* and *FL-1* signals of each GUV suspension were measured as a technical triplicate (see representative counter maps in *Fig. S5* and *S6*). As a detection limit, $1x10^5$ events was set. The raw data was exported as listmode files and processed with FlowJo. Only GUVs with a diameter >4 µm were considered in our analysis and all events showing a fluorescence signal were gated and defined as a GUV population. The electronic volume values (*EV)* were exported to excel, transformed via Eq. 1 into the electronic radius (*Er*), and standardized by Eq. 2 utilizing fluorescent-labeled standard beads (NIST traceable latex particle, indicated as STD in Eq. 2 with a nominal diameter of 10 µm. The ratio ($10\ \mu m/ER_{STD}$) between the known diameter (10 µm) and the measured *Er* for the standard (ER_{STD}) was used to transform the non-specified electronic volume of GUVs to the diameter in µm.

$$Er = \sqrt[3]{\frac{3}{4\pi}EV} \quad \text{(Eq. 1)}$$

$$d_{GUV} = \frac{Er_{GUV}}{Er_{STD}} \cdot d_{STD} \quad \text{(Eq. 2)}$$

The scale was verified with standard particles of 20 µm (see *Fig. S7*), and the accuracy tested. The size of all the measured GUVs was categorized into five different groups for clarity, and the yield was expressed as GUVs per µL.

Access to FlowJo was kindly provided by Sander van Kasteren from the bio-organic synthesis group, Leiden University.

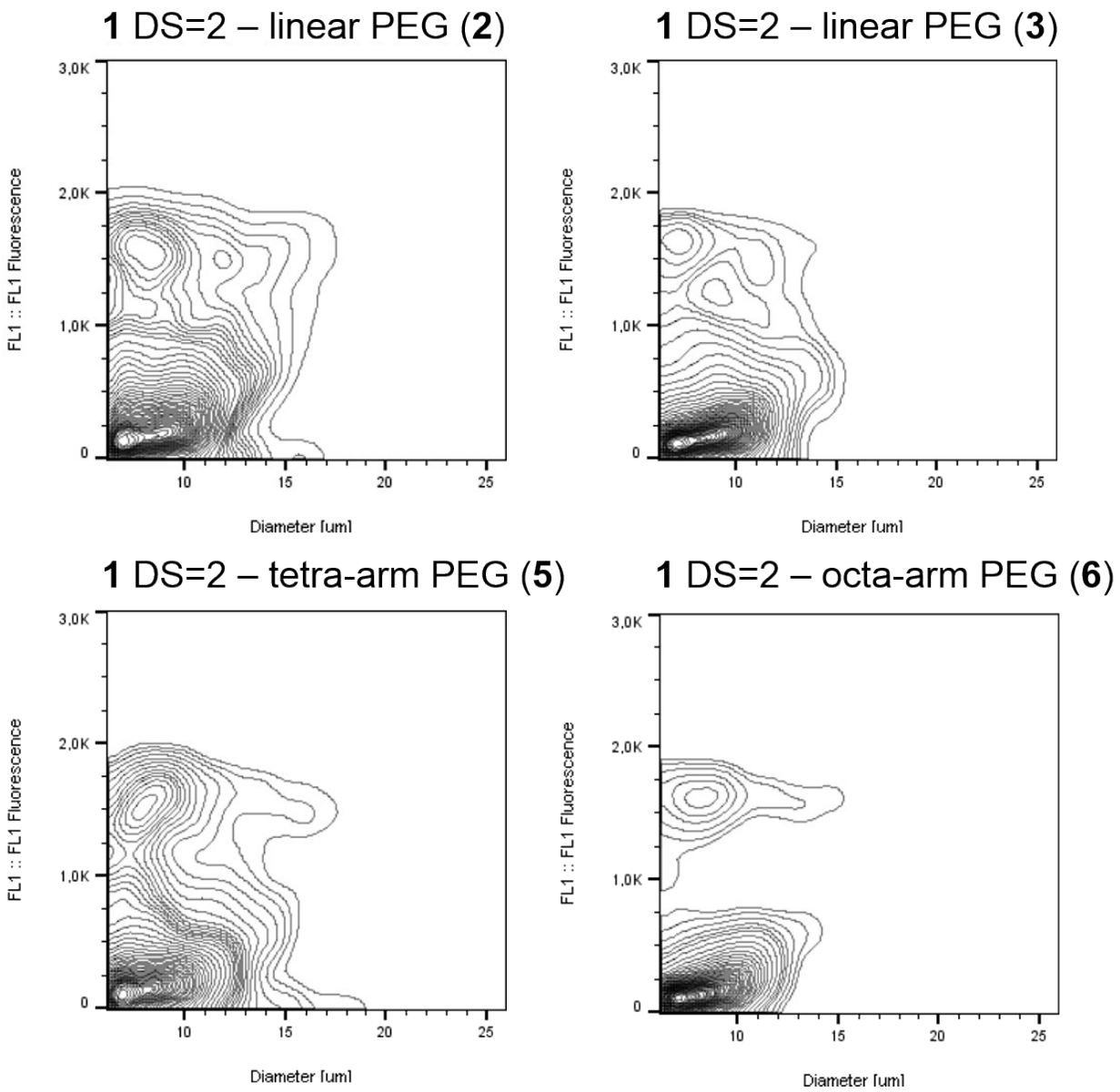

Fig. S5 The effect of the crosslinker in the production and size of GUVs as measured by flow cytometry. Contour maps of the relative frequency of GUVs populations with the lipid composition POPC/Cholesterol/PEG 2000-PE (75:20:5 molar ratio, 14 mM) fluorescently labeled with DOPE-NBD (0.7 mol%) and prepared in DexPEG hydrogel substrates with **1** DS = 2 and PEG crosslinkers **2**, **3**, **5** and **6**.

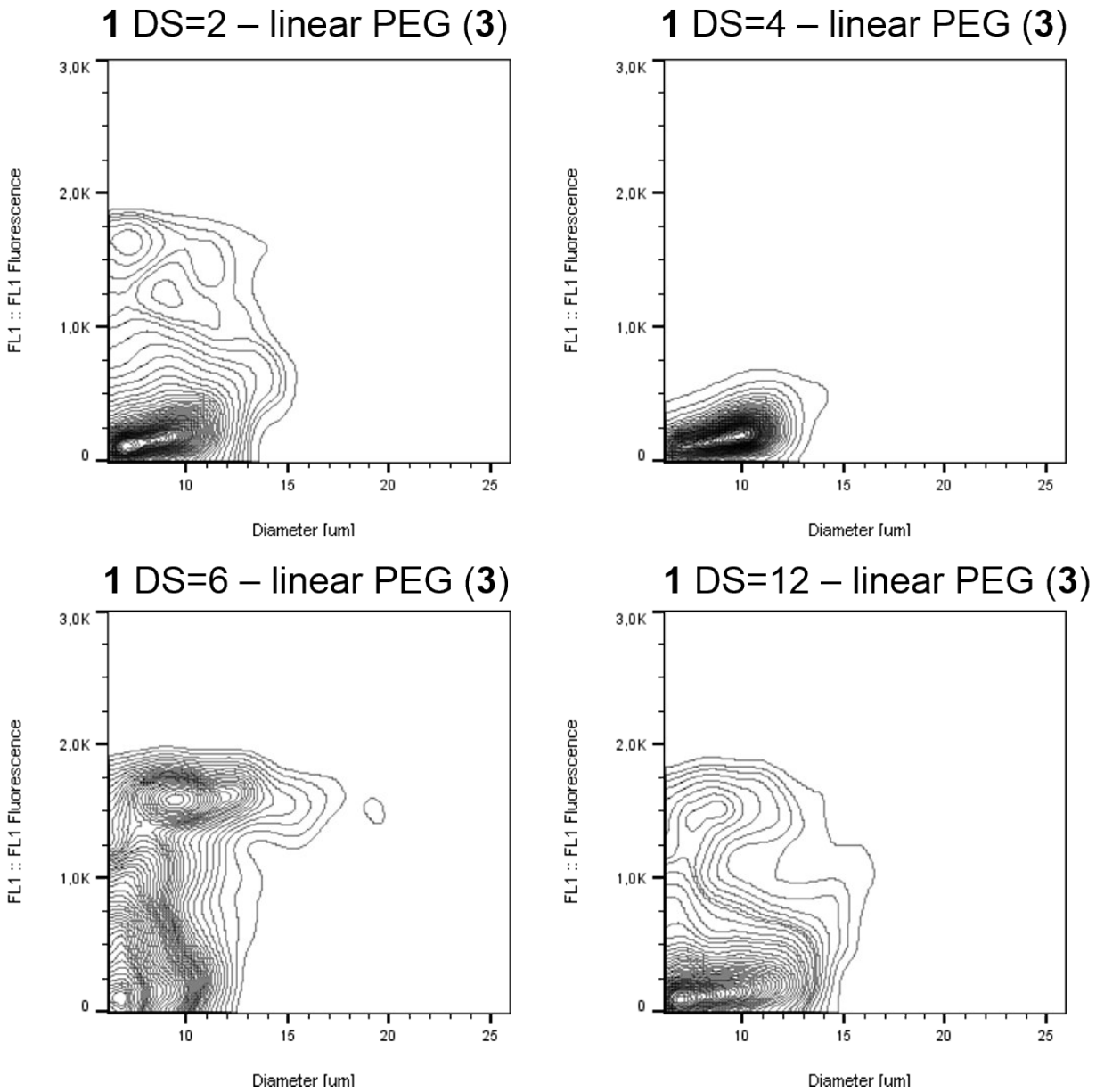

Fig. S6 The effect of the degree of substitution (DS) in the production and size of GUVs evaluated by flow cytometry. Contour maps of the relative frequency of GUVs populations with the lipid composition POPC/Cholesterol/PEG 2000-PE (75:20:5 molar ratio, 14 mM) fluorescently labeled with DOPE-NBD (0.7 mol%) and prepared in DexPEG hydrogel substrates with **1** DS = 2, 4, 6, 12 and linear PEG crosslinker **3**.

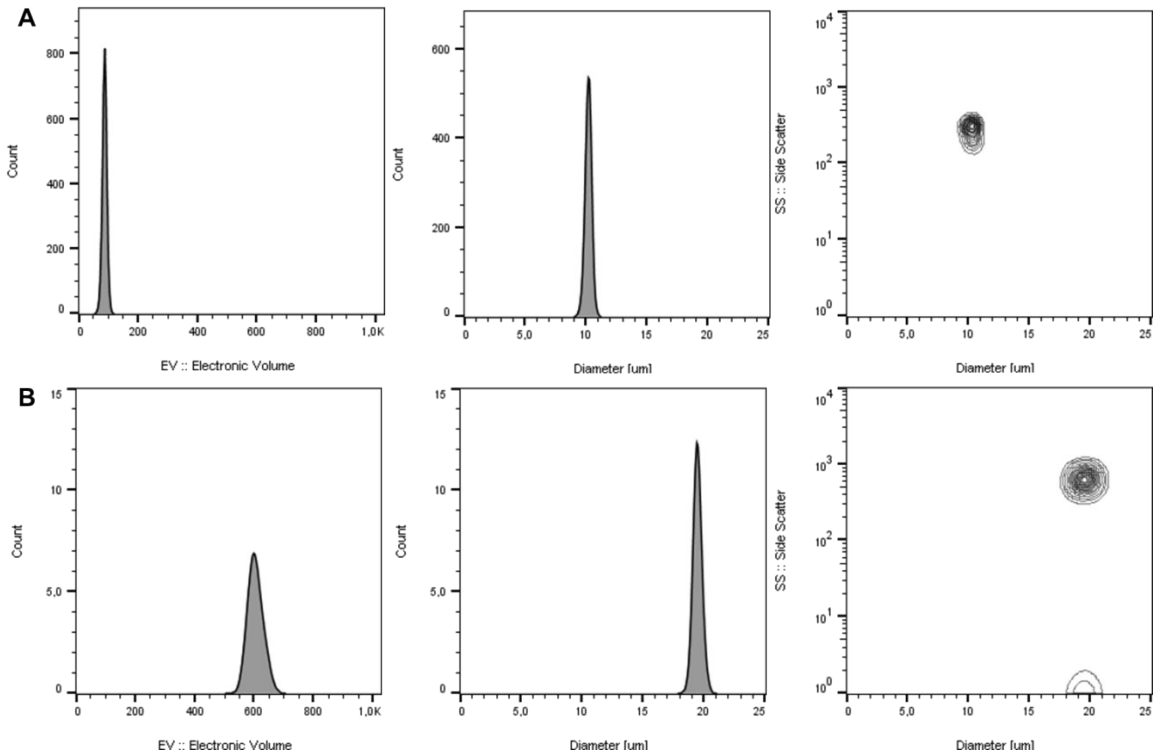

Fig. S7 Verification of the diameter with NIST Traceable Latex Particles Standards. A) Histogram and contour map for latex particles with standard nominal of size 10 µm and B) Histogram and contour map for latex particle with standard nominal of size 20 µm.

Differential Scanning Calorimetry (DSC). Temperature scans were performed in a Discovery DSC from TA instruments. Temperatures from -50 to 50 °C were scanned at a heating rate of 10 °C/min. Two sequential heating traces were performed and recorded. No differences were observed between the first and second heating run. DSC traces for the first heating run are presented in *Fig. S8*. The baseline was subtracted and the heat flow signal was normalized for all samples. A well-defined melting transition (T_m) was detected for pure DOPC lipid at -6 °C (black trace). This value is in good agreement with the value reported for hydrated DOPC (*ca* 3 H_2O).[7] *Fig. S8A* shows the DSC traces for the dry DexPEG hydrogel film (*Fig. S8*, *gray*) and the dry hybrid DOPC – DexPEG hydrogel film (*Fig. S8*, *blue*). Thermal analysis indicates slight interaction between DOPC and DexPEG by the displacement of DOPC T_m to -12 °C and PEG T_m from 45 °C to 42 °C. In *Fig. S8B* the strong interaction of DOPC lipid with PEG hydrogel is detected by 1 °C displacement of PEG T_m and the depression of the DOPC melting transition.

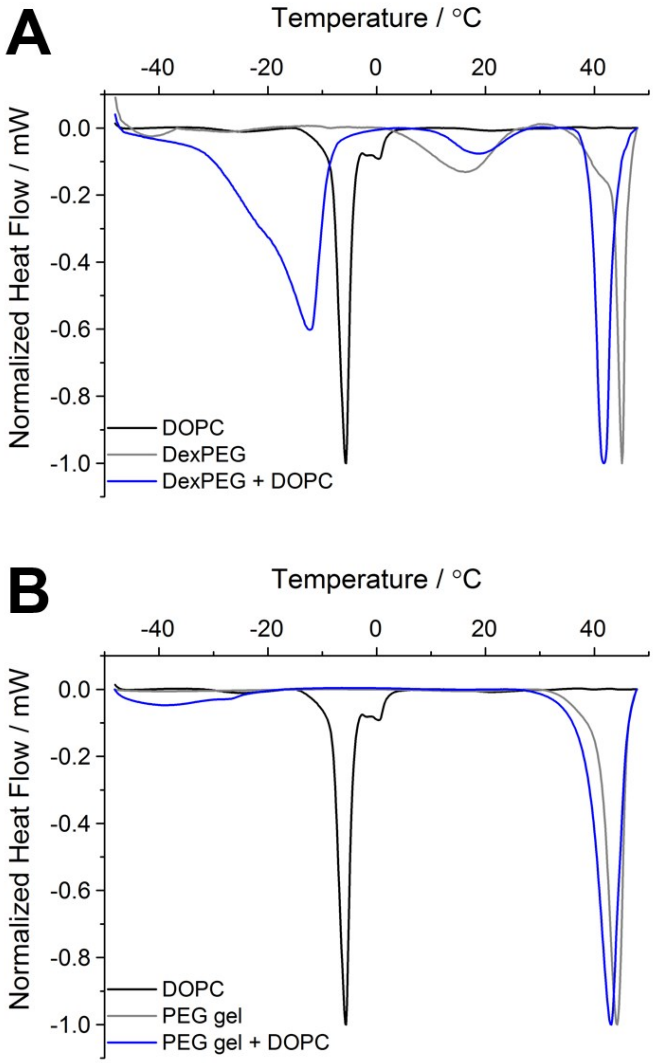

Fig. S8 Thermal analysis of DexPEG and PEG hydrogels. A) Normalized thermograms of DexPEG, DOPC and DexPEG - DOPC. B) Normalized thermograms of the PEG gel, DOPC and PEG gel - DOPC. The baseline was subtracted for all the traces.

Confocal and differential interference contrast (DIC) Imaging. Spinning-disc confocal microscopy was performed on a TI-Eclipse inverted microscope (Nikon, Japan) equipped with a 16-bit Cascade II 512 EMCCD camera (Photometrics, USA) and a CSUX confocal head (Yokogawa, Japan). Illumination was provided by a 50 mW solid-state laser at 561 nm (Coherent Inc., Germany) and the objective used was a 60× NA1.43 Plan-Apo Nikon oil-immersion objective. DIC imaging was performed on an Axio Observer (Zeiss, Germany) equipped with a Hamamatsu CMOS camera (Hamamatsu, Japan). Illumination was provided by a halogen lamp 12V 100W using a differential interference contrast prism with polarizer (Zeiss, Germany) and the objective used was a 20x NA0.8 Plan-Apo Zeiss objective.

Surface roughness was primarily identified through inspection of micrographs. Image fields were qualitatively classified into "rough" and "smooth" regions; *Fig. 5* in the main text gives representative examples of each type of surface. The two types of regions could also be seen upon visual inspection of the films without magnification. The *Fig. S9* shows film-coated glass mounted in observation chambers. The hazy, opaque regions on the glass surface correspond to rough film. The qualitative phenomenon described (*i.e.* vesicles size depending on surface roughness) was reproducible observable in three samples for each of the DexPEG species formed from tetra-arm and octa-arm PEG, a total of six samples.

Fig. S9 DexPEG-coated glass mounted in sample holders. The opaque, hazy regions on the glass correspond to the rough film regions shown in *Fig. 5B* and *5C* of the main text.

Polymersomes encapsulation into GUVs. The extent of free-floating GUVs containing polymersomes were evaluated by confocal laser scanning microscopy (CLSM). The re-hydration of the dry lipid film with PBS on hybrid polymersome - DexPEG hydrogel substrates produced GUVs containing polymersomes in their aqueous inner volume, *Fig. S10A*. Conversely, the re-hydration of a dry lipid film on DexPEG hydrogel substrates with a polymersome solution did not lead to their encapsulation into GUVs, *Fig. S10B*.

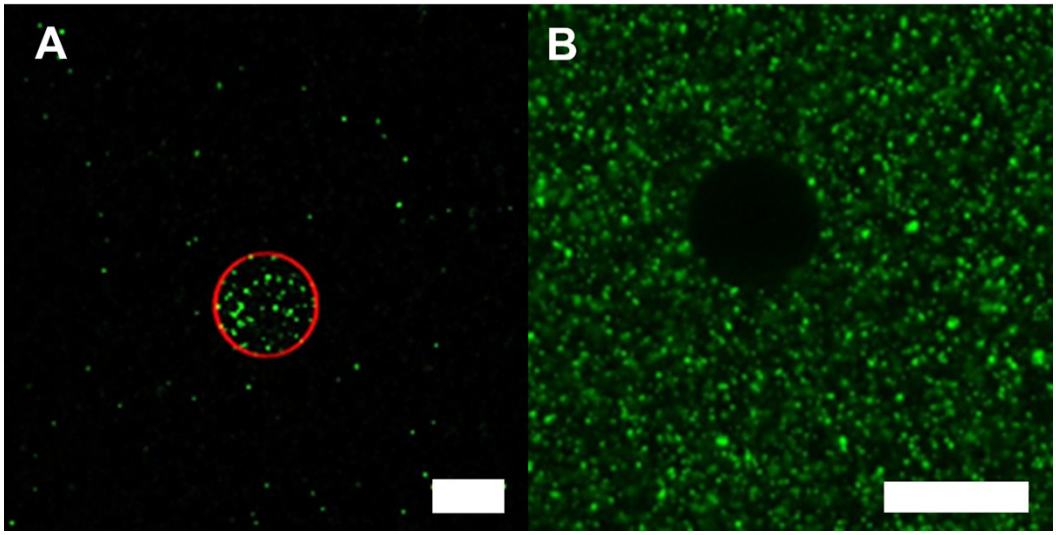

Fig. S10 Free-floating GUVs with the lipid composition DOPC : DOPE : cholesterol (50 : 25: 25 mol%) in PBS. A) GUV formed on the hybrid polymersome – DexPEG hydrogel substrate. The GUV membrane is labelled with PE (Lissamine Rhodamine B) and the polymersomes with ATTO488 for dual colour imaging in a fluorescence microscope. Scale bar is 50 µm. B) GUVs formed on a DexPEG hydrogel substrate re-hydrated with a solution of polymersomes. Encapsulation of polymersomes does not occur. Scale bar is 50 µm.

Dex-PEG hydrogel films were examined for the preparation of GUVs with different lipid compositions. Encapsulation of fluorescently-labeled polymersomes in the GUV aqueous inner volume is shown in *Fig. S11*. Inclusion of PEGylated lipids was intended to promote the steric repulsion of polymersomes and negatively charged lipids to promote the electrostatic repulsion of polymersomes during vesicle growth. All the tested lipid compositions produced both effective polymersomes encapsulation and GUVs formation.

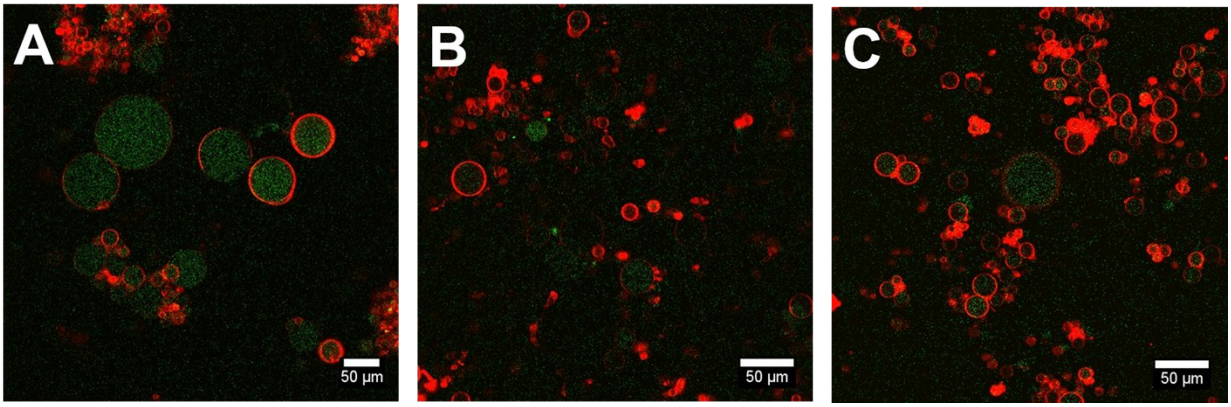

Fig. S11 Free-floating GUVs containing polymersomes in the aqueous inner volume of different lipid compositions. A) GUVs with the lipid composition POPC : POPG (90 : 10 mol%). B) GUVs with the lipid composition POPC : POPG (50 : 50 mol%). C) GUVs with the lipid composition DOPC : DOPE : cholesterol : PEG2000-PE (49.5 : 25 : 25 : 0.5 mol%). The membrane of the GUVs is labelled with PE (Lissamine Rhodamine B) and the polymersomes with ATTO488 for dual colour imaging in a fluorescence microscope.

3. References

1. R. M. de Figueiredo, P. Oczipka, R. Frohlich and M. Christmann, *Synthesis-Stuttgart*, 2008, 1316-1318.
2. S. F. M. van Dongen, W. P. R. Verdurmen, R. J. R. W. Peters, R. J. M. Nolte, R. Brock and J. C. M. van Hest, *Angew Chem Int Edit*, 2010, **49**, 7213-7216.
3. R. J. R. W. Peters, M. Marguet, S. Marais, M. W. Fraaije, J. C. M. van Hest and S. Lecommandoux, *Angew Chem Int Edit*, 2014, **53**, 146-150.
4. C. W. H. a. H. W. R, *Google Patents*, 1971.
5. H. M. Shapiro, *Practical Flow Cytometry*, Wiley, 2005.
6. H. M. Shapiro, John Wiley & Sons, Inc, 2005, pp. 1-60.
7. A. S. Ulrich, M. Sami and A. Watts, *Bba-Biomembranes*, 1994, **1191**, 225-230.